

A029146

REPRODUCTION
BY PERMISSION OF
INFORMATION CANADA

RESEARCH AND DEVELOPMENT BRANCH
DEPARTMENT OF NATIONAL DEFENCE
CANADA

DEFENCE RESEARCH ESTABLISHMENT OTTAWA

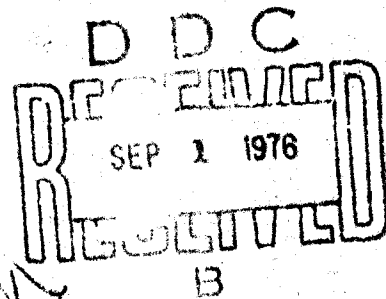
DREO TECHNICAL NOTE NO. 76-13
DREO TN 76-13

THERMAL IMAGING FOR CLOTHING RESEARCH. A REVIEW OF THE LITERATURE

by

D.J. Hudson

Best Available Copy



PROJECT NO.
76-13

MAY 1976
OTTAWA

~~SERVICE D'INFORMATION SCIENTIFIQUE POUR LA DÉFENSE~~

Ministère de la Défense Nationale
Ottawa, Ontario, Canada
K1A 0K2

Les documents ci-joints vous sont transmis à titre gracieux. Vous pouvez en disposer comme vous l'entendez; ne les renvoyez pas au Service d'information scientifique pour la défense. Un accusé de réception n'est pas nécessaire.

76-101

DEFENCE SCIENTIFIC INFORMATION SERVICE

Department of National Defence
Ottawa, Ontario, Canada
K1A 0K2

The enclosed complimentary documents are for your use and disposal. Please do NOT return them to the Defence Scientific Information Service. Please do not acknowledge receipt.

UNCLASSIFIED

REPORT NO:

DREO Technical Note No. 76-13

PROJECT NO:

79-01-04

TITLE:

Thermal Imaging for Clothing Research
A Review of the Literature

AUTHOR:

D.J. Hidson

DATED:

May 1976

SECURITY GRADING:

UNCLASSIFIED Initial distribution
August 1976

- 2 - DSIS
 - Plus distribution
 - 1 - DSIS Report Collection
 - 1 - Document Section (Microfiche)
- 1 - GRAD
- 1 - DSTI
- 1 - DCGEM
- 1 - DREO
- 1 - DRES
- 1 - SA/FMC

- 1 - DGMDP
- 1 - DLR-5
- 1 - ORAE
- 1 - DCIEM
- 1 - CDLS/L, CDR
- 1 - CFNBS School

- 1 - NRC/CISTI
- 3 - Senior Standardization Representative US Army
 - Plus distribution
 - 3 - DDC/NTIS

BRITAIN
Ministry of Defence
6 - DRIC

RESEARCH AND DEVELOPMENT BRANCH

DEPARTMENT OF NATIONAL DEFENCE
CANADA

DEFENCE RESEARCH ESTABLISHMENT OTTAWA

⑨ TECHNICAL NOTE, NO. 76-13

⑥ THERMAL IMAGING FOR CLOTHING RESEARCH -
A REVIEW OF THE LITERATURE.

⑩ by
D. J. / Hidson
Environmental Protection Section
NBC Defence Division

⑪ May 76

⑫ 44p.
⑭ DREO-TN-76-13

ACCESSION for	
NTIS	White Section <input checked="" type="checkbox"/>
DOC	Buff Section <input checked="" type="checkbox"/>
UNANNOUNCED	<input type="checkbox"/>
JUSTIFICATION.....	
BY.....	
DISTRIBUTION/AVAILABILITY CODES	
Dist.	AVAIL. and/or SPECIAL
A	

PROJECT NO.
79-01-04

76-074

RECEIVED APRIL 1976
PUBLISHED MAY 1976
OTTAWA

404576


13

TABLE OF CONTENTS


	<u>Page</u>
<u>ABSTRACT/RÉSUMÉ</u>	(iii)
1. <u>INTRODUCTION</u>	1
1.1 THEORETICAL BACKGROUND	1
2. <u>EMISSIVITIES OF MATERIALS AT ROOM TEMPERATURE</u>	2
2.1 THEORETICAL	2
2.2 MEASURED VALUES OF EMISSIVITY	3
3. <u>TRANSMITTANCES OF VARIOUS MATERIALS</u>	5
3.1 TRANSMITTANCE OF GLASSES	5
3.2 INFRARED OPTICS	6
4. <u>EMISSIVITY</u>	7
4.1 EMISSIVITY OF EXPERIMENTAL BLACK RADIATORS	7
4.2 EMISSIVITY AND THE ENVIRONMENT	10
4.3 EMISSIVITY OF SKIN	11
5. <u>REFLECTANCES</u>	14
5.1 REFLECTANCES OF FABRICS	14
6. <u>INFRARED DETECTORS</u>	15
6.1 LEAD SULFIDE, LEAD SELENIDE, INDIUM ANTIMONIDE, GERMANIUM AND MERCURY CADMIUM TELLURIDE	15
6.2 SIGNAL-TO-NOISE RATIOS IN BOLOMETERS AND QUANTUM DETECTORS...	17

TABLE OF CONTENTS - Continued

	<u>Page</u>
6. <u>INFRARED DETECTORS</u> (continued)	
6.3 THERMOCHROMIC MATERIALS - CUPROUS MERCURIC IODIDE	13
6.4 PYROELECTRIC DETECTORS	19
6.5 N-COLOR MERCURY CADMIUM TELLURIDE DETECTORS	22
7. <u>THERMAL IMAGING</u>	22
7.1 REFERENCE TEMPERATURE DEVICES	22
7.2 THERMAL IMAGING SYSTEMS	24
8. <u>APPLICATIONS OF THERMAL IMAGING</u>	27
8.1 MEDICAL DIAGNOSIS	27
8.2 DESIGN OF ARCTIC CLOTHING	29
9. <u>REFERENCES</u>	30

ABSTRACT

This paper reviews the literature relating to thermal imaging (particularly real-time thermal imaging), photoconductive, photovoltaic and pyroelectric infrared detectors and the application of thermal imaging to the design of Arctic clothing. The application of thermal imaging to medical diagnosis and non-destructive testing is also discussed.

RÉSUMÉ

Dans le présent rapport, on fait la revue de la documentation ayant trait à l'obtention de thermogrammes (surtout instantanés), aux détecteurs photoconducteurs, photovoltaïque et pyroélectriques d'ondes infrarouges, ainsi qu'à l'application de la thermographie à la conception de vêtements qui seront utilisés dans l'Arctique. Le rapport traite également de l'utilisation des thermogrammes pour les diagnostics médicaux et les essais non destructifs.

PRECEDING PAGE BLANK NOT FILMED

1. INTRODUCTION

The purpose of this review is to survey the literature relating to thermal imaging, (particularly real-time thermal imaging), photoconductive, photovoltaic and pyroelectric detectors and the application of thermal imaging to the design of better protective clothing for extremely cold environments.

Present day thermal imaging is mainly concerned with the radiation from bodies in the near and medium infrared bands. The energy in these bands is determined by characteristics of the body such as temperature, emissivity, and reflectance. The signal that can be developed from this energy is dependent on the transmission characteristics of the medium, on the quality of the infrared optics used to form an image, and on the sensitivity of the detectors used.

Accordingly, this review examines relevant literature dealing with the radiation laws on which thermal imaging is based, the emissivities and reflectances of materials, particularly clothing materials, infra-red optics, detectors used in relevant wave-bands, and applications of thermal imaging to military clothing problems. For brevity, a list of the symbols and abbreviations used in this review . . given in Appendix A.

1.1 THEORETICAL BACKGROUND

All bodies at temperatures above absolute zero radiate electromagnetic energy. The lower the temperature of a body, the less energy is radiated, and the longer is the wavelength of that energy. At temperatures encountered on the Earth's surface, most of the energy is radiated in the infrared part of the spectrum between $1\text{ }\mu\text{m}$ and $10^4\text{ }\mu\text{m}$. (For comparison, the visible spectrum lies between 0.4 and $0.7\text{ }\mu\text{m}$). Since the quantity and wavelength of radiation is a function of temperature, it is possible to measure the temperature of objects by observing their output of radiation.

Modern techniques began essentially in 1879 with the discovery of the Stefan radiation law, which states that the total emissive power of a radiating body is proportional to the fourth power of temperature: that is,

$$E(T) = \sigma T^4 \text{ (}\sigma \text{ is a constant).}$$

This applies only to bodies which radiate the maximum possible energy at each wavelength. Such bodies are called full radiators or "blackbodies". However, all real bodies do not behave exactly as these ideal "blackbodies" but radiate partially as functions of wavelength and temperature. This means that they are possessed of an emissivity ϵ and for them $E(T) = \epsilon \sigma T^4$.

Subsequent to Stefan's discovery came the development of the relation between radiant energy intensity and the wavelength at which it was emitted. This culminated in Planck's law. Planck's spectral distribution of emissive power is given by the formula

$$E(\lambda) = 2\pi hc^2 \lambda^{-5} (e^{hc/\lambda kT} - 1)^{-1}.$$

At each temperature each curve exhibits a maximum at a certain value of λ which shifts towards shorter values of wavelengths as the temperature rises.

When the above formula is integrated over all wavelengths, the total hemispherical emitted power is obtained which is found to be proportional to the fourth power of the absolute temperature. The constant of proportionality is the Stefan-Boltzmann Constant. The value of this constant is found to be

$$\sigma = 2\pi^5 k^4 T^4 (15c^2 h^3)^{-1}.$$

The Planck distribution function has a pronounced maximum, at a certain value λ_m of the wavelength λ . At this point

$$T\lambda_m = 2.898 \text{ mm K and}$$

λ_m decreases with increasing temperature. This latter relationship is Wien's Law.

2. EMISSIVITIES OF MATERIALS AT ROOM TEMPERATURE

2.1 THEORETICAL

In thermal imaging with human subjects we are often dealing with very small temperature differences coupled with high backgrounds. In a paper on low-temperature pyrometry (1), T.P. Gill considered some of the problems encountered in these situations. For an object ΔT warmer than its surroundings at T the difference in energy radiated is:

$$\Delta E = \sigma(T + \Delta T)^4 - \sigma T^4$$

$\approx 4\sigma T^3 \Delta T$ (taking the derivative of the Stefan-Boltzmann Law). For this

approximation to be accurate to within 1% when $T = 300$ K, ΔT must be less than 2°C .

If the absolute temperature of the body is required, the emissivity, ϵ , of the surfaces in question must be known. Since infrared detectors are sensitive to the energy incident upon them, a change in emissivity of the emitter will be indistinguishable from a change in absolute temperature. To determine the absolute temperature, an experiment can be envisaged in which T_S , T_R , and T_B , are the absolute temperatures of the surroundings, the infrared receiver and the background respectively with ϵ_S , ϵ_R , and ϵ_B the respective emissivities.

After setting up the energy equation, that is, the net energy incident on the receiver in terms of the energy from the background, surroundings and receiver, the change in background emissivity $\Delta\epsilon_B$ in T_B , is found to be given by:

$$\Delta T_B (\Delta \epsilon_B)^{-1} = (T_B^4 - T_S^4) (4 \epsilon_B T_B^3)^{-1}.$$

Thus the extent of a change in the emissivity depends on the "contrast" between the body and the environment.

The assumption that the radiation from a body originates at the surface was examined. It was found that for small temperature gradients (of the order of 10°C cm^{-1}) almost all the radiant energy was emitted from the outermost $10 \mu\text{m}$ of the body. Thus, the assumption that thermal radiation from the human body originates at the outer layer of skin was verified.

2.2 MEASURED VALUES OF EMISSIVITY

An experimental approach to emissivities was made by D. Weber (2). The author pointed out that spectral emissivities are usually made at high temperatures (with respect to the environment) so that the spectral emissivity may be written

$$\epsilon(\lambda, T) = W(\lambda, T) [W_b(\lambda, T)]^{-1}$$

where $W(\lambda, T)$ is the power radiated per unit wavelength interval per unit area at T K, and $W_b(\lambda, T)$ is the same for a blackbody under identical conditions, where $W_b(\lambda, T)$ is expressed by Planck's Law

$$W_b(\lambda, T) = c_1 \lambda^{-5} (e^{c_2/\lambda T} - 1)^{-1}.$$

The difficulty with low-temperature measurements is that when the spectrometer observes a specimen at a temperature at which its emitted flux is about equal to, or even less than, that from the spectrometer or the environment, more

involved equations have to be considered such as

$$W(\lambda, T) = \epsilon(\lambda, T)W_b(\lambda, T) + [1 - \epsilon(\lambda, T)] \bar{W}(\lambda, T')$$

where the first term is the power emitted by the specimen and the second term is the contribution from the environment reflected into the spectrometer by the specimen.

Ordinarily, the radiation is optically chopped and mechanically rectified, and the radiation from the specimens is compared to that from a chopper (usually a shiny metal sheet or mirror). Since the emissivity of the chopper may vary with temperature changes, it is desirable to have the chopper term vanish from the equation if possible.

Two methods were considered. First, it is assumed that a flat, specularly reflecting, opaque specimen is emitting at a fixed wavelength λ at two different temperatures, T_1 and T_2 and T is the environment. Thus

$$\begin{aligned} W(\lambda, T_1) - W(\lambda, T_2) &= \epsilon(\lambda, T_2)[W_b(\lambda, T_1) \\ &- \bar{W}(\lambda, T)] - \epsilon(\lambda, T_2)[W(\lambda, T_2) - \bar{W}(\lambda, T)]. \end{aligned}$$

It was then assumed that

$$\epsilon(\lambda, T_1) = \epsilon(\lambda, T_2) = \epsilon_\lambda$$

hence the background term $\bar{W}(\lambda, T)$ was eliminated. This resulted in an expression

$$\epsilon(\lambda, T) = \frac{W(\lambda, T) - \bar{W}(\lambda, T')}{W_b(\lambda, T) - \bar{W}(\lambda, T')}.$$

If $T \gg T'$, \bar{W} may be considered negligible. Cooling of the environment might be used to advantage to reduce the contribution of $\bar{W}(\lambda, T')$.

Voltage signals from the specimen and blackbody, recorded at T_1 and T_2 were recorded and equations set up assuming $V(\lambda, T) \propto W(\lambda, T)$. The constant of proportionality was eliminated and ϵ_λ found from:

$$\epsilon_\lambda = \frac{V(\lambda, T_1) - V(\lambda, T_2)}{V_b(\lambda, T_1) - V_b(\lambda, T_2)}$$

T_1 and T_2 for the observations were not necessarily the same as those temperatures at which the instrument was calibrated. Other calibration temperatures T_3 and T_4 could be used as long as there was no change in the gain of the amplifier or slit width during a series of measurements. Small temperature differences were used throughout.

A variation on the above consisted of using two different specimens of the same material at temperatures T_1 and T_2 respectively and having two independent blackbody sources at T_1 and T_2 also. The four sources were

scanned sequentially. The signals from the spectrometer give

$$\begin{aligned} V(\lambda, T_1) - V(\lambda, T_2) &= \Delta V = K \epsilon_\lambda [W_b(\lambda, T_1) - W_b(\lambda, T_2)] \\ V_b(\lambda, T_1) - V_b(\lambda, T_2) &= \Delta V_b = K [W_b(\lambda, T_1) - W_b(\lambda, T_2)] \end{aligned}$$

so

$$\Delta V / \Delta V_b = \epsilon_\lambda$$

From these ratios the emissivity was deduced. Also, the only values needed were one accurate emissivity value and three ratios.

3. TRANSMITTANCES OF VARIOUS MATERIALS

3.1 TRANSMITTANCE OF GLASSES

For all optical systems, and particularly infrared systems, finding materials with good transmittance is a problem. G.W. Cleek, J.J. Villa and C.H. Halmer (3) measured the refractive indices of several optical glasses in the 0.43 to 4.25 μm band. (The 2-5 μm band is one to which InSb photo-detectors are most sensitive).

Thirteen sample glasses were used and those glasses containing any significant amount of boron were rejected as boron-containing glasses show very pronounced absorption bands in the 3 μm area. Refractive index and transmittance were measured, the latter for different thickness of the material.

The measured values of refractive index for flint glasses all showed curves of the same shape, dropping rapidly in the visible spectrum (0.5 to 0.7 μm) and falling less sharply out to 4 μm . The transmittances were measured for 12 glasses and the results displayed for 3 different thickness of material. The general curves followed similar patterns, all thicknesses of the glass showing 90% transmittance out to 2 μm . Beyond 2 μm the increases in thickness cut down transmission significantly (to 75%) and at 2.8 μm sharp drops in transmittance were observed for the 1.0, 2.5 and 5.0 mm thickness. The curves traversed a wide shallow dip at 3.5 μm rising to a small maximum at 4 μm , dropping to zero transmittance for all thickness at 4.5 to 5.0 μm .

As optical glasses tested were made in a gas-fired furnace it was concluded that water in the glass contributed to the sharp absorption at 2.8 μm and beyond.

As thermal radiation from human skin is situated in the middle infrared band ($5\text{ }\mu\text{m} - 15\text{ }\mu\text{m}$) it would be desirable to have optical materials that are transparent in this band.

P.S. McDermott, R.L. Powell and E.R. Stack (4) measured some relevant optical constants of an arsenic-sulfur-thallium glass system. Because these glasses have very low melting points and high fluidities between 125°C and 350°C , this permits glasses to be molded with Teflon dies.

Measurements were made with one piece of material of composition As: S: Tl of 30:34:36. The glass was hot-pressed into shapes required. The temperature of the pressing surfaces was controlled by thermocouples. The disks were 1.2 cm in diameter with a thickness variation of $\pm 5\%$. A Perkin-Elmer model 21 infrared spectrometer containing sodium chloride optics was used for spectral scanning.

The composite material was found to have a transmittance of 70% out to $8\text{ }\mu\text{m}$ increasing to 83% at $11\text{ }\mu\text{m}$. This declined to about 50% at $20\text{ }\mu\text{m}$. R , n , (the refractive index), and k , (the extinction coefficient) were measured at $1\text{-}\mu\text{m}$ intervals and the results processed on a computer. The refractive index curved down from 3.4 at $2\text{ }\mu\text{m}$ to 1.7 at $14\text{ }\mu\text{m}$, rising again to 2.5 at $20\text{ }\mu\text{m}$.

3.2 INFRARED OPTICS

Because thermal radiation is emitted by all objects at room temperature, including optical materials, the choice of material is more difficult in infrared optics than in visible optics.

The infrared spectral emittance of some important materials used in infrared systems was measured by D.L. Stierwalt (5).

The measurement process compared radiation from a sample with that from a blackbody at the same temperature. The sample compartment and monochromator formed an isothermal compartment at temperature T_p . The signal from the detector consisted of emitted, reflected and transmitted radiation and a term accounting for the chopper as it intercepted the beam. A blackbody source was used as a comparison to the sample.

Three spectrophotometers were used, each for a different part of the spectrum. These instruments carried the slit width to maintain a constant output from the detector. The slit and wavelength drive programs were recorded on magnetic tape with a blackbody in place of the sample. This produced a full-scale deflection on the chart recorder corresponding to an emissivity of 1.0. The blackbody was then replaced by the sample and the same program used to control the slit width and wavelength drives, thus eliminating variation in amplifier gain, detector response, etc. The sample and standardizing blackbody were heated or cooled by thermal conduction from a copper or aluminum block.

The Irtran materials produced by Kodak were examined in the range 3.5 - 45 μm at 77 K. A 2-mm-thick specimen of Irtran 1 showed almost zero emittance out to 6 μm , an emittance of nearly unity from 7 to 16 μm and then dropping again to 0.05 at 20 μm . It rose again rapidly at longer wavelengths.

A similar sample of Irtran 2 at 4.2 K, 77 K, and 373 K showed an identical profile but shifted towards the longer wavelengths, the emissivity being <0.2 out to 14 μm rising sharply to 0.85 then slowly to 0.95 at 29 μm . A sample of Irtran 5 showed very low emissivity out to 8 μm , a plateau of more than 0.95 between 10 and 13 μm , a plateau of almost zero between 16 and 25 μm and a rising profile beyond that. All the materials showed a temperature dependence of emissivity, Irtran 2 being transparent even beyond 70 μm . The low emittance bands were where the materials were transparent.

It was observed that use of room-temperature data for calculating optical quantities at other temperatures produced unreliable results.

4. EMISSIVITY

4.1 EMISSIVITY OF EXPERIMENTAL BLACK RADIATORS

In order to measure most values in infrared optics it is necessary to have a standard source of radiant energy.

To measure emissivity it is necessary to have a standard for comparison, that standard being commonly known as a blackbody radiation source. Various types of sources are discussed in a paper by C.S. Williams (6). In classical physics a blackbody consisted of an enclosure with walls with high emissivity and a tiny opening to prevent much radiation entering the hole. A useful blackbody must have an opening relatively large - this results in a departure from a true blackbody. In the paper by Williams, the general integration theory of cavities was discussed first.

To obtain an expression for the apparent emissivity of a cavity the following expression was written down

$$\psi(\alpha_1) = \epsilon + (1 - \epsilon) \int_S \psi(\alpha_2) K(\alpha_1, \alpha_2) d\alpha_2$$

where

ψ = the fraction of full blackbody radiant emittance,
 $\sigma T^4 \psi(\alpha_1)$ = radiant emittance in watts per unit area leaving the
 elemental area $d\alpha_1$,

ϵ = emissivity, assumed uniform over the surface,

σ = the Stefan-Boltzmann Constant,

$\sigma T^4 \psi(\alpha_2)$ = radiant emittances in watts per unit area leaving the elemental area $d\alpha_2$,

$T = K$

$K(\alpha_1, \alpha_2) d\alpha_2$ = radiant power from α_2 reaching α_1 for the case when $\sigma T^4 \psi(\alpha_2) = 1$,

$\epsilon \sigma T^4$ = radiant emittance in watts from a unit area.

This expression described the amount of radiation leaving a point, both emitted and reflected. This problem has been solved approximately by Buckley (7). Cylindrical, conical and biconical cavities have been used as blackbody radiation sources and numerical integrations were carried out for cylindrical cavities. For a wall emissivity of $\epsilon = 0.9$, a cylindrical cavity had an effective emissivity of greater than 0.999 for a length-to-radius ratio greater than 5.

The Gouffé theory of cones, cylinders and spheres was also discussed in this paper. Gouffé derived an expression for the emissivity of a cavity without integral equations. He supposed that unit quantity of radiant energy entered the cavity whose walls had reflectivity ρ . An amount is diffusely reflected by the opposite wall and an amount $\rho\Omega/\pi$ passes out again. Thus to a first approximation $(1 - \rho\Omega/\pi)$ is the effective emissivity. (Ω is the solid angle subtended by the opening at the point of reflection.) Uniform illumination of the cavity was assumed and a second reflection results in $\rho^2[1 - \rho\Omega/\pi]s/S$ leaving the cavity, where s is the opening area and S the cavity area including s . In a spherical cavity the good approximation $s/S = \Omega/\pi$ was made. After many reflections it was found that the flux leaving the cavity was

$$\rho \frac{s}{S} + \rho^2 [1 - s/S] s/S \{1 + \rho + \rho^2 [1 - s/S]^2 + \dots\}.$$

This gave the reflectivity of the cavity. Thus the value ϵ_0 derived was

$$\epsilon_0 \approx 1/[1 - s/S + s/(\epsilon S)],$$

which may be written in the form

$$\epsilon_0 = \epsilon(1 + k),$$

from which k can be computed. This method did not give such accurate values as the integral equation method, but agreement was quite reasonable.

The De Vos theory for specular reflection was also discussed. The assumption of diffuse reflection did not need to be made. Because of the angular dependence, the theory became quite complicated. An expression derived for the emissivity of the cavity was difficult to evaluate even for the simplest geometries.

It was concluded that the values of effective emissivities were probably not better than $\pm 1\%$ and that cavities designed for experimental use are over designed where accuracy is required. Computers may be used to solve Buckley's integral equations numerically and so provide a comparison with the De Vos method.

The most convenient design shape for sources of infrared radiation is the cylinder. An exhaustive study of the thermal radiation characteristics of cylindrical enclosures was presented in a paper by E.M. Sparrow, L.U. Albers and E.R.G. Eckert (8).

The case of very long holes has been analysed by other workers but the investigation of Sparrow et al. centered around short holes. The physical system consisted of a cavity of length L and diameter d with isothermal walls. Radiant interchange within the cavity was analysed numerically for L/d values ranging from 4.0 to 0.25 and emissivity values of 0.9, 0.75 and 0.5.

The analysis began with the radiant energy flux balance at a general point x_0 . The flux balance at a particular point was written as

$$B(x_0) = \epsilon \sigma T^4 + \rho H(x_0)$$

where $\rho = 1 - \epsilon$,

B = the radiant energy leaving per unit time per unit area,

H = rate at which energy is incident per unit area, and the two unknowns being B and H .

From these equations the effective emissivities of various sizes of cylindrical cavities were computed for various surface emissivities. Also, equations were set up to compute the radiant heat loss from various parts of the cavity and these, too, had to be solved numerically. For cylinders of length L and diameter d , graphs were displayed of $\epsilon_a(x)$, the apparent emissivity against x/d , where x was the distance down the cylinder from the mouth. The apparent emissivity of the end disk is the most interesting as this is what a detector "sees" when looking into the cavity.

It was observed that $\epsilon_a(r)$, where r is a radial distance from the centre of the end disk, did not become uniform or even nearly so until the apparent emissivity approached unity closely e.g. for $\epsilon = 0.9$, $L/d = 2$, x/d , $\epsilon_a(2d) = 0.998$ and $\epsilon_a(r)$ varied between 0.994 at $r/R = 1$ and 0.993 at $r/R = 0$.

As the hole became shorter, the distribution of ϵ_a over the end disk became less and less uniform and ϵ_a decreased in magnitude. For any L/d the nonuniformities increased as ϵ decreased. As an example, when $\epsilon = 0.5$, $L/d = 0.25$, ϵ_a varied from 0.569 to 0.732 over the disk.

Conversely, it was found that $\epsilon_a(x)$, the apparent emissivity of the walls varied very little as L varied. As for $\epsilon_a(r)$, the apparent emissivity of the end disk, this was found to vary significantly over the disk surface for $L/d < 1$ (e.g. from 0.73 to 0.57 for $\epsilon = 0.5$ and $L/d = 0.25$) but the value of $\epsilon_a(r)$ was essentially flat at $L/d \geq 3$ and $\epsilon \geq 0.5$ so for short holes it was found that ϵ_a cannot be assumed constant over the walls and as the surface

emissivity ϵ decreased, longer holes had to be considered to enable the assumption $\epsilon_a(r) = \text{constant}$ to be valid.

Results were also presented graphically for the heat loss from the cylindrical walls and separately from the end disk. For x/d and $L/d > 1$, the heat losses from the walls were almost identical for all the emissivities considered. For long holes, there was very little heat loss from either the end disk or from parts of the walls distant from the mouth. As far as the total heat loss from the cavity was concerned it increased with increasing emissivity but the increase was by no means proportional to the emissivity. For shallow holes, $L/d = 0.25$, heat transfer from the cavity was found to be $0.6569 \sigma T^4 \pi R^2$, as compared with $0.5 \sigma T^4 \pi R^2$ from a disk of $\epsilon = 0.5$ - a full 30% increase. This result could be important in the design of spacecraft - particularly with regard to the effects of meteorite bombardment.

Although cavities can be constructed to emit nearly as blackbodies, it so happens that in the $8 \mu\text{m}$ to $13 \mu\text{m}$ waveband the human skin approximates a black radiator. When infrared imaging or radiometry is performed on the human body the intensity of the radiation emitted corresponds almost exactly with the temperature of the skin, for although $E = \epsilon \sigma T^4$, $\epsilon \approx 1$.

4.2 EMISSIVITY AND THE ENVIRONMENT

Variations in emissivity are of great importance in thermal imaging because infrared detectors are sensitive to the product of emissivity and temperature to the fourth power and not to emissivity or temperature separately.

If a surface, such as the surface of the Earth, possesses various gradations in emissivity the infrared radiance of the surface can provide useful information, particularly if it is displayed as a map. The usefulness of this approach has been demonstrated by J.H. McLerran (9). In this paper the remote thermal sensing of the environment is described in relation to desert terrain and polar ice.

Aerial surveys were done over some high temperature terrain in the vicinity of Yuma, Arizona. Two observations were made immediately:

- (1) the imagery did display the terrain features such as hills and roads and an old alluvial fan; and
- (2) it was important to know the time of day that the images were taken.

Infrared images were shown of the same piece of terrain at five different times ranging from mid day to midnight. During the night the alluvial fan showed up as cold surface while the gullies and depressions were warm. In the morning, the temperature profiles were reversed, the desert surface appearing very warm and the gullies cold. Vegetation appeared warm during the night and cold during the day.

Hot springs and geysers were also surveyed in Yellowstone National Park. A image was displayed which showed the hot springs area to be lighter in contrast to the surroundings but the individual springs and geysers were not resolved. However, a image taken at 1010 hours showed the hot springs contrasted strongly to the Firehole River, the springs being much hotter than the river. Again the diurnal variation in contrast was present. A photograph taken 0627 hours showed the bodies of water hotter than the background and not noticeably different from the hot springs.

The imagery detected a thermal anomaly not consonant with surface features. The anomaly turned out to be present in a rhyolite dome, 1 mile across rising to 800 feet above the surroundings countryside. It was found that the thermal anomaly was caused by warm springs issuing from the base of the hill.

Some remote sensing projects were also carried out in the Arctic. Photographs were taken of sea ice in the Gulf of St. Lawrence and in Arctic waters. A comparison of visible photographs and infrared images was presented. Visible photographs taken in April 1962 show thin winter ice which was grey. Snow-covered ice appeared nearly white. In the infrared, the tones were reversed, the thin ice appearing very light, or warm, and the snow covered ice appearing black, or cold. The infrared image of the sea ice illustrated correlation between ice thickness and the apparent temperature of the surface. The ability to discriminate between various types of sea ice was demonstrated but the interpretation of the results depended very much upon the prevailing conditions.

4.3 EMISSIVITY OF SKINS

R. Elam, D.W. Goodwin and K. Williams (10) have investigated some optical properties of the human skin. They measured reflectance and transmittance of a specimen of human skin with a Perkin-Elmer type 21 spectrometer and plotted the calculated emissivity. For the experiments, a specimen of epidermis was sandwiched between two sapphire plates.

Reflectance measurements covered the range out to 2.7 μm . In between 0.8 and 1.4 μm the reflectivity fell from 0.65 to 0.1 and remained at this level out to 2.7 μm . Transmissivity measurements indicate that between 3 and 6 μm , the calculated emissivity is greater than 0.7 and for wavelengths beyond 6 μm the epidermis acts essentially as a blackbody emitter.

Further work on the same subject was performed by D. Mitchell, C.H. Wyndham and T. Hodgson (11). They pointed out that 90% of the thermal radiation emitted from the human body lies in the 6 - 42 μm band. At the time of writing (1967) this was not easily investigated by infrared quantum detectors as HgCdTe and various other compounds had not been developed. Some authors had reported emissivity values of 0.99 and higher with the added conclusion that only radiation from the surface of the skin is important. However, other equally involved work by Büttner and Eckoldt had produced

values of 0.954 ± 0.004 . Also, some of the latest work has again shown the influence of blood flow on emissivity. These differences are important as the difference between 0.99 and 0.95 in emissivity can result in an error of as much as 1°C in temperature measurement which is far greater than that permitted by modern standards of skin temperature measurement. The paper by Mitchell et al. attempted to resolve some of these contradictions.

Their method was based on the fact that the rate of transfer of radiant energy (Q) between the skin target and the radiometer depends on the skin temperature T_s and the radiometer temperature T_r . The Stefan-Boltzmann law was utilized:

$$Q = A\sigma\epsilon_s\epsilon_r(T_s^4 - T_r^4)$$

where ϵ_s and ϵ_r are the emissivities of the skin and radiometer, σ the Stefan-Boltzmann constant and A an area factor determined by the field of view of the radiometer. The radiometer produced an output $\phi = CQ$ (C a constant) and the skin temperature was held constant while the radiometer temperature was varied giving

$$\phi = \phi_0 - CA\sigma\epsilon_s\epsilon_r T_r^4$$

where ϕ_0 was a constant. The regression equation of ϕ on T_r^4 was thus linear with gradient $-CA\sigma\epsilon_s\epsilon_r$. This gradient was compared with that produced by a blackbody under identical conditions and the ratio ϵ_s/ϵ_b was extracted, ϵ_b being the emissivity of the blackbody.

A sample of skin was mounted in the aperture of a re-entrant conical blackbody. All the measurements were performed inside a climatic chamber where the air and wall temperatures were kept close to the values for human skin. A horizontal current of air was blown across the skin to minimize natural air currents.

The radiation from the skin and the blackbody was measured alternately and the temperature of the sensor of the radiometer was increased in steps of 3°C . The radiometer sensing unit consisted of a radiation thermocouple in an evacuated capsule with a rock salt window. The device was sensitive to wavelengths of up to $20\text{ }\mu\text{m}$ so it accepted 75% of the radiation emitted by the skin sample. Twenty-four measurements were made on 7 different samples consisting of skin from different races including Bantu, Caucasian and Cape colored (mulatto).

The results confirmed earlier work extending back to Hardy in the 1930's that the emissivity of human skin (in the infrared) is 0.99 or higher. The weighted mean for all measurements on all samples produced the value of 0.997 ± 0.001 . A value of 0.997 was obtained for the total normal emissivity of the skin from each of the racial groups. Some values of emissivity greater than unity were presented but this was because of the random scatter of results about a number very close to unity.

Two reasons were advanced for the high values of emissivity. First, the surface of the skin is not smooth but is patterned with ridges, furrows and pores. Also, on top of this roughness, there is a second order of

roughness at the cellular level, where there is a constant erosion of dead cells from the surface. Another possible explanation lay in the high water content of the skin. Water has a high emissivity even in very thin films but even then, values of 0.95 and 0.97 are quoted for water which are still lower than the value for skin. Dehydration should thus result in a lower emissivity value for skin and this was found to be the case.

Some explanations were also advanced for the low values of emissivity obtained by other workers. Büttner's result of an emissivity equal to 0.954 ± 0.004 in the 0.3 to 50 μm band was attributed to an interaction between the skin and the radiometer when the radiometer was close to the skin and at a different temperature from it. Other workers, Gärtner and colleagues, measured the skin temperature by thermocouple and radiometer and there is always a difference between these readings. It was surmised that the difference observed here was due to a change in skin temperature in the presence of the radiometer rather than a change in emissivity.

The authors thought any change in properties between excised and living skin was unlikely because the infrared emissions took place from the surface of the skin, the cells of which are largely dead, or at least very inert.

A description of the technique behind this kind of measurement (emissivity measured by a radiometer) is contained in a book on Behavioral Temperature Regulation edited by Hardy, Gagge and Stolwijk (12). A chapter by D. Mitchell is devoted to the technique of measuring the emissivity of human skin by means of a radiometer.

Because infrared radiometers constitute the most accurate instruments for measuring surface temperature, a detailed and fairly intimate knowledge of the optical and various emissive properties of the human skin is required. The method used was the same as that described in the previous paper (11). The instrumentation, the radiometer, was newly designed by the author to eliminate some of the problems encountered in measuring the emissivity of living skin.

The radiometer had certain conditions to fulfil:

1. It had to be non-selective, i.e. sensitive to all wavelengths of infrared radiation.
2. It had to have an output proportional to the rate of radiation exchange and the detector characteristics could not be influenced by its own temperature.
3. It had to have a very narrow acceptance angle.
4. The temperature of the sensing element had to be measurable, controllable and variable.
5. It had to measure 0.1°C .

The radiometer accepted radiation in a beam of circular section 25 mm in diameter. It had a barrel 300 mm long containing collimators to eliminate all but paraxial rays. The novel aspect lay in the chopper design. The main fault of other radiometers was that the emissivity of the chopper did not stay sufficiently close to zero for any length of time, that is the emissivity rose because of atmospheric corrosion. Here, by introducing a 45° mirror made of the same material as the chopper - gold on polished glass - the radiometer "saw" itself reflected off the chopper or the target reflected off the mirror.

The output ϕ could then be written

$$\phi \propto \epsilon_d \epsilon_t (1 - \epsilon_m) \sigma(T_t^4 - T_d^4) + \epsilon_d \epsilon_m \sigma(T_m^4 - T_d^4) - \epsilon_d \epsilon_c \sigma(T_c^4 - T_d^4)$$

where the subscripts d, t, m and c refer to the detector, target, mirror and chopper respectively. If $T_m \approx T_c$ and $\epsilon_m \approx \epsilon_c$ the chopper has no appreciable effect on the output ϕ even if $\epsilon_t \neq 0$. Provided that the mirror and chopper were at approximately the same temperature and age, the effects of the chopper temperature were eliminated. If no mirror were included in the system the output becomes

$$\phi \propto \epsilon_d \epsilon_t \sigma(T_t^4 - T_d^4) - \epsilon_d \epsilon_c \sigma(T_c^4 - T_d^4)$$

where the chopper has a definite effect if $\epsilon_c \neq 0$.

The sensing element contained 300 radiation thermocouples coated with silicon carbide which was highly absorbing in this wavelength range. The output from this element was amplified by a low-noise high-gain preamplifier. The total amplification was 1.5×10^6 .

The process of measurement took about 10 minutes over which period the output rose from -1.5 mV to +2.0 mV and the detector temperature dropped from 36°C to 28°C. As the detector temperature dropped, the difference between detector and target temperature became greater and thus the rate of radiation transfer became greater. They found that the emissivity of skin was within 1/2% of unity.

5. REFLECTANCES

5.1 REFLECTANCES OF FABRICS

The paper reviewed here contains descriptions and uses of infrared and thermal imaging which are of great relevance to the design of Arctic

clothing and thermal protection. The amount of heat absorbed and/or reflected by the colors of various materials was described by H.F. Greenler and F.J. O'Neil (13). Measurements of radiant-energy reflectance from human skin showed that the least reflection, and thus maximum absorption, was in the 500 - 600 nm range of the visible, which incidentally is where the solar spectrum is at a maximum. Thus the visible reflectance of a material such as skin is as important as its infrared reflectance.

The radiant-energy reflectance of several samples of worsted fabrics of a variety of colors was measured. The measurements were performed using a General Electric Recording Photoelectric Spectrophotometer with a 10 nm wavelength band and measurements covered the region 400 to 1000 nm. The light colored fabrics (white, yellow, blue, tan, grey and green) showed reflectances from between 70% and 38%. Medium-colored fabrics (red, brown, green, blue and gray) measured between 45% and 28% and the dark-colored fabrics (green, brown, blue, and black) between 25% and 5%. The infrared reflectance varied between 80% from the lightest colors down to 22% with the darkest color where as the visible reflectance was only 45% at the lightest end dropping to about 3% at the darkest.

Other factors besides radiant-energy reflectances, such as water and air permeability affect the comfort level of fabrics greatly. Also, the type of construction and finish on the cloth will affect how much radiant energy is absorbed in the fabric and how much is transmitted through the skin. But as practical experience shows, the lighter colors are best for warm weather clothing as they reflect most of the infrared energy as well as most of the visible.

Intermittently during a 3-month period, several persons wore two shirts of different radiant-energy reflectances. They were then asked as to which felt the cooler of the two shirts. The results indicated that the lighter colors usually felt cooler but for two shades of the same visible color, infrared differences made one shirt appreciably cooler than the other.

6. INFRARED DETECTORS

6.1 LEAD SULFIDE, LEAD SELENIDE, INDIUM ANTIMONIDE, GERMANIUM AND MERCURY CADMIUM TELLURIDE

On the more quantitative side of thermal imaging, a 1968 paper (14) by M. Smollet describes some of the properties of infrared radiation detectors. Detectors are now available that cover the entire wavelength spectrum from visible to microwave. Several detector materials were discussed in this paper, including lead sulfide, lead selenide and indium antimonide.

Lead sulfide cells were made by 2 processes: evaporation on to a substrate or by chemical deposition. The spectral response was the same for both types but the time constant of the evaporated cell was four times less than the chemical. Detectors as small as 50 μm could be fabricated but only by the chemical deposition method. The maximum detectivity was quoted as $>5 \times 10^{10} \text{ W}^{-1} \text{ cmHz}^{1/2}$ at room temperature a value which increased with cooling. The detectivity is defined as the reciprocal of the noise equivalent power (NEP). The quantity quoted here is D^* which is the signal-to-noise ratio when one watt is incident on a detector having a sensitive area of 1 cm^2 and the noise is measured with an electrical bandwidth of 1 Hz. Thus D^* is really a normalized detectivity.

Lead selenide, a detector used in the 4- μm region, has been superseded by indium antimonide because of the latter's shorter time constant.

Indium antimonide can be made for use in the photoconductive or photovoltaic mode, the photoconductive mode possessing the fastest response owing to minimal capacitance. The sizes of detectors can extend down to 50 μm . Their optimum operating temperature is 77 K.

Most infrared detectors work at low temperatures in order to minimize background noise. Some detectors have been used at room temperature where the spectral response peaked at about 6.5 μm . However, since these detectors possess a 50 ns time constant, their suitability for high speed operation has been realised in the detection of 10 μm energy from CO_2 lasers.

Indium antimonide detectors work best around 77 K. Their detectivity was reported as $>4 \times 10^{10} \text{ W}^{-1} \text{ cmHz}^{1/2}$ and their sensitivity as $2 \times 10^4 \text{ VW}^{-1}$. A detectivity of $>3 \times 10^{11} \text{ cmHz}^{1/2} \text{ W}^{-1}$ was reported when a cooled aperture stop was used in front of the cell.

For the detection of radiation out to 25 μm either copper- or mercury-doped germanium was used. The impurity concentration was very low - around 10^{15} cm^{-3} .

The copper-doped germanium required cooling to <10 K and liquid helium at 4.2 K was used for this purpose.

The wavelength range that it was sensitive to was 2 to 25 μm with a peak at 15 μm . The detectivity and time constant were $2 \times 10^{10} \text{ W}^{-1} \text{ cmHz}^{1/2}$ and <300 ns respectively.

However, the mercury-doped germanium could also be operated at higher temperatures up to 40 K which enable it to be used with closed cycle heating engines. Despite this advantage, the wavelength range was limited to 2 to 14 μm . Like indium antimonide, great variations in sizes of the cells were possible.

At ordinary temperatures encountered on the surface of the Earth, the wavelength at which the maximum intensity of infrared radiation is emitted is at 10 μm . A 1:1 molar combination of mercury telluride and cadmium telluride will produce a compound having peak photoconductive response at 10 μm when cooled to 77 K using liquid nitrogen. The property of photoconductivity

is an intrinsic one and so this compound can operate at fairly high temperatures. The detectivity has been made as high as $10^{10} \text{ W}^{-1} \text{ cmHz}^{1/2}$ with resistances of 300Ω and time constants of 1 ns. This material is very versatile because its maximum sensitivity is at the wavelength of maximum thermal emission at 300 K.

Detection of the far infrared has always been difficult because of the low temperatures required for the detectors. Boron-doped germanium at 40 K will detect out to $100 \mu\text{m}$. Beyond $100 \mu\text{m}$ (0.1 mm) detection of infrared is difficult. N-type indium antimonide is used with very low impurity concentrations to produce ionization energies of 10^{-3} eV . If "pumped" liquid helium is used to reduce the detector temperature to 1.5 K and a 6 kG magnetic field used, the response may be extended to 8 mm ($8,000 \mu\text{m}$). The detectivity is high ($10^{11} \text{ W}^{-1} \text{ cmHz}^{1/2}$) and the response time short (0.2 ns).

Attention was brought to a new type of bolometer using the ferroelectric effect. Certain of these materials show a strong correlation between changes in polarization with temperature near their Curie point. These changes give rise to surface charges so that when the material is contained between two conducting electrodes, its behavior is that of a variable capacitance when infrared radiation is incident upon it. The time constants are of the order of 1 ns with detectivities of $2 \cdot 10^9 \text{ W}^{-1} \text{ cmHz}^{1/2}$. This type of detector has no cooling requirement. A more complete description may be found in a later review (18).

6.2 SIGNAL-TO-NOISE RATIOS IN BOLOMETERS AND QUANTUM DETECTORS

These high-speed infrared detectors can be put to great use in thermal imaging systems. A paper by B.R. Holeman and R.G.F. Taylor (15) reviews some of the most important theory behind the design of a thermal imaging system. The basic properties of infrared radiation, the Stefan-Boltzmann law and the Planck law are discussed. The various types of quantum and bolometric detectors are discussed as well.

The signal-to-noise ratios of bolometers and photon detectors were discussed in some detail. Bolometric detectors are sensitive to all incoming radiation, irrespective of wavelength. The limiting noise process for these detectors is shot noise on the photon signal (as opposed to radar where the limit is Johnson noise, kTB). Other noise is also present, including thermal noise from the atmosphere. However, the best signal-to-noise ratio would be $3.3 \times 10^4 \text{ }^\circ\text{C}^{-1}$ which is about two orders of magnitude better than present detectors are capable of.

Photon detectors respond to the incident photon flux up to a long-wavelength limit. An ideal photon detector would have a uniform photon response independent of wavelength and unit quantum efficiency up to this limit. On this basis, a similar expression was derived for the signal to noise ratio in photon detectors. Because there was some wavelength dependence, it was shown that in the $8 - 14 \mu\text{m}$ band, the signal-to-noise ratio is about four times its value at $5 \mu\text{m}$.

Some infrared pictures were displayed that had been taken with an infrared linescan device developed by the Royal Radar Establishment, Malvern.

The infrared pictures showed many temperature sensitive gradations which varied diurnally so that interpretation of infrared pictures was very difficult unless the conditions at the time of exposure were known. Another imaging method mentioned involved covering a large area with a thin bolometric layer of a pyroelectric material. The pyroelectric image generated by the thermal image could be scanned by an electron beam and the image displayed on a television screen. This process has been demonstrated with pyroelectric triglycine sulfate.

A fairly general review of the devices available (in 1967) for thermal imaging was presented in a paper by C. Maxwell Case and B.V. Barlow (16). Their paper describes the various systems used in infrared imaging (involving quantum detectors, bolometric detector design criteria etc.) which have been discussed in several other papers.

6.3 THERMOCHROMIC MATERIALS - CUPROUS MERCURIC IODIDE

Another approach to thermal imaging, but more akin to photography, involves the use of thermochromic cuprous mercuric iodide, Cu_2HgI_4 . A paper by J.S. Chivian et al. (17) reports current research on this material. Cuprous mercuric iodide exhibits hysteresis phenomena in reflectance vs temperature, conductivity vs temperature, and volume vs temperature. At room temperature the material is bright red, but, upon heating to 66°C , it changes to black. To use the material for imaging purposes a paint is usually made up using powdered Cu_2HgI_4 . On heating, the red-black transition occurs around 66°C and the black-red transition on cooling occurs over a range of temperature around 50°C . The changes were carried out as near isothermally as possible and it was found that there was no difference in the transition temperatures if Cu_2HgI_4 was in powder form, solution or suspension. Furthermore, once a thermal image had been made, it would remain indefinitely provided that the compound was stored at a constant temperature.

A curve of reflectance against temperature was displayed for a mixture of silicone varnish and Cu_2HgI_4 and the reflectance was arbitrarily chosen to be unity at 40°C . Upon slow heating (1°Cmin^{-1}) the reflectance decreased slowly to 0.8 at 65°C and then very sharply dropped to 0.15. Above 70°C it remained relatively constant. When cooled, the reflectance remained low until 62°C was reached where it began rising and below 50°C it rose rapidly to 0.85. If the material was left for several days at room temperature the reflectance value would return to unity. If reheating were commenced again immediately, a slightly different hysteresis loop was followed, the change being in the initial to final reflectance ratio. To obtain reproducible results the material was first cycled through several loops. The loops were similar to hysteresis loops for ferromagnetic materials and were useful for recording heat sinks, such as a fingerprint, by cooling from a temperature above the black to red transition temperature.

Clearly, for thermal imaging application the speed at which an image can be stored on the material is of critical importance. Photographs were displayed of spots $4\text{ }\mu\text{m}$ across, made on cuprous mercuric iodide by 50-ns exposures to a 5-mW He-Ne laser beam. This corresponded to an energy density of about 90 mJ cm^{-2} , quite a bit more than would have been required by the specific heat calculations, but attributable to the metal heat sink. For bias temperatures of $63 - 64^\circ\text{C}$, temporary images were formed. At powers above 500 mW cm^{-2} , semipermanent images were formed. This meant that the temperature of the material had to be raised to 70°C to erase the image.

The resolution obtained using thermochromic materials was examined and it was found that a He-Ne laser could draw a line $10\text{ }\mu\text{m}$ wide. The authors suggested a $1\text{-}\mu\text{m}$ resolution would be attainable with refinements in grain size.

In their discussion of the mechanisms of thermochromic materials, particularly cuprous mercuric iodide, the days-long memory of the material was supposed to be a frozen-in disordered phase with a very long relaxation time. Metastability of this frozen-in phase was also thought to be the key to the reflectivity inversion.

6.4 PYROELECTRIC DETECTORS

Pyroelectric detectors form a novel method of thermal imaging. Unlike quantum detectors, they are bolometric, that is, sensitive to all wavelengths of infrared, and do not have to be cooled. A paper by R.W. Astheimer and F. Schwartz (18) describes pyroelectric detector methods. They pointed out that the ultimate detectivity of a thermal detector is determined by the random temperature fluctuations of the absorbing element and is dependent only on the element itself and the readout mechanism. Sensitivity in pyroelectric detectors is achieved only if temperature noise is predominant, which is not the case in detectors such as resistance bolometers which are limited by Johnson noise. In the pyroelectric detector, the functional parameter is capacitance - from which Johnson noise is absent.

Pyroelectric materials are ferroelectrics that exhibit a temperature dependence of ferroelectricity. This dependence can be used as a readout facility and is particularly attractive as no biasing current or voltage is required. A typical detector consists of a $6.3\text{ }\mu\text{m}$ -thick Mylar film with a metallised upper surface stretched over a support ring. Conducting electrodes are evaporated onto the pyroelectric material (triglycine sulfate) one side of which is then attached by means of conducting cement to the Mylar film. An absorbing "black" is applied to the other surface.

The responsivity and thermal time constant of such a detector used in the T-6 Thermograph was described. As with other bolometers, the detectivity was almost a constant. However, it did decrease with increasing frequency as a result of the dissipation factor. This factor was a result of the loss

tangent α . In low-speed video systems, the frequency response must be maintained down to very low frequencies. $1/f$ noise was the most bothersome in other types of infrared detectors but as no biasing voltages were needed with the pyroelectric detector, the noise from these sources was eliminated. Also, the responsivity increased with $1/f$ down to the thermal time constant break of 0.06 Hz where it was 10^6 VW^{-1} . A network was necessary in the video system to produce a flat frequency response to signal. This network caused the gain to be very low at low frequencies, thus suppressing $1/f$ amplifier noise and maintaining constant responsivity - a highly desirable situation.

In the Thermograph, a single mirror served for scanning a photo-recording. A germanium lens imaged the scene on to the detector plate. The horizontal line scan was $3\text{-}1/3 \text{ lines s}^{-1}$ and was accomplished by a torque motor driving against an air dashpot. Uniformity of scanning velocity is absolutely critical when photographs are involved as the film response depends on the product of spot intensity and dwell time. After one line was scanned, a relay was tripped allowing the mirror to return quickly to its starting position during which time a blackened vane of constant temperature was inserted in front of the detector. The vertical scan time was 30 s. The vertical scanning could be stopped at a point to allow faster scanning of one part of the target. Black-and-white or color records could be produced.

Correct electronic handling of output signal from the detector was important. The low-capacitance detector required a low-capacitance, low-noise, high-impedance input on the amplifier which was accomplished by means of a field-effect transistor. This was mounted with the detector in an evacuated chamber. Controls were kept to a minimum, brightness and temperature range being the only important ones.

The possible uses and applications of thermography have been illustrated in various other papers reviewed by Astheimer and Schwartz herein. Several thermograms were displayed, electrical circuits, radiant heater, human subjects with temperature scales of 5°C to 100°C full scale. Overworked electrical circuits in power lines were shown to be significantly warmer than their surroundings.

Until recently, the detection of electromagnetic radiation in the far infrared has been very difficult as the frequencies involved are too high for microwave techniques and too low for optical techniques. Thermal detectors, i.e. bolometers, have been the best means of detecting far infrared radiation. A new bolometer for this wavelength region, which consists of a single crystal chip of p-type undoped thallium selenide (TlSe) as the temperature sensitive element, is described by P.S. Nayar (19). The optical system contains a brass pipe of 1-cm internal diameter and an exit aperture of 1-mm diameter. The detector is mounted below this light pipe, the top of which is covered with a 0.2-mm thick black polyethylene sheet which acts as a long-wave band pass.

The carrier concentration in the bolometer element was $1.2 \times 10^{17} \text{ cm}^{-3}$ and the chip measured 6 mm x 1 mm x 1 mm. No blackening was used. The electrical connections were of 0.12 mm gold wire soldered to the ends of the element with indium solder. The vacuum can containing the package was totally immersed in liquid helium. A low noise FET preamplifier at room temperature was used to amplify the signal from the bolometer.

At these very low temperatures, the effect of background radiation was an apparent increase in the bath temperature. To reduce this noise the operating temperature of the bolometer should be below 0.5 K.

As a corollary to the pyroelectric thermal imaging device, mention should be made of a pyroelectric energy meter designed by J.L. Lachambre (20) for the detection of high-peak-power CO₂ laser pulses.

The detector consisted of a diverging lens and a large sensing head mounted on a common axis separated by a cavity whose internal walls were highly reflecting. The radiation entered the cavity after passing through the diverging lens and almost all of it was absorbed by the detector element. The diverging lens was a 5-cm focal length sodium chloride lens (transparent to a wide range of infrared radiation) which was coated with a $\lambda/4$ layer of sodium fluoride for antireflection properties. The detecting element was a lead zirconate titanate ceramic ground down to 0.25 mm thickness and coated with silver. The absorbing material coating the ceramic was lamp- or gold-black. All these additions reduced the power reaching the detecting element by a factor of 50.

The mechanical construction was quite simple. A block of aluminum 1.27 cm thick acted as the heat sink on to which the ceramic was fixed by a conducting glue. On the free side of the ceramic a silver electrode was vacuum deposited and on top of that a layer of lampblack.

The thermal characteristic of the detector was derived by solving the heat conduction problem for a thin slab with one face kept at zero temperature and the other exposed to a known flux. If the output radiation is in the form of a step function, the mean temperature of the slab follows a curve of the $(1 - e^{-t/T})$ shape. The thermal time constant is much longer than the pulse length from a laser. The risetime of the electrical output signal was determined by the time constant of the absorbing lampblack surface, which was about 1 ms. Times of the order of 1 μ s might be achieved with gold-black films.

The decay time could be adjusted by means of a shunt resistor in the circuit. A decay time ten times longer than the rise time was desirable. However, it was the peak of the signal which gave the energy contained in the pulse.

As the pyroelectric crystal was also piezoelectric, errors could creep in if mechanical vibrations were allowed to disturb the detector. Expansion of the ceramic itself due to the incident radiation could be a source of error. This error was minimized by reducing the thickness of the pyroelectric sheet. The piezoelectric factors were dependent on the thickness of the ceramic sheet whereas the pyroelectric factors were completely independent of this.

Calibration was carried out with a 2-J, 2-MW TEA CO₂ laser and the detector exhibited linearity of response over 3 orders of magnitude up to 2J. A value of about 40 VJ⁻¹cm⁻² was obtained, but because of the difference between manufactured ceramic sheets, each detector had to be calibrated independently.

6.5 N-COLOR MERCURY CADMIUM TELLURIDE DETECTORS

A recent development with quantum detectors has been the manufacture of N-color mercury cadmium telluride detectors (21). Depending on the molar fraction of mercury or cadmium in the compound, the wavelength at which it is most sensitive can be varied. By altering the concentrations of mercury and cadmium the width of the band gap is changed, thus changing the photon energies to which the material is sensitive. In order to build an N-color detector, material was made up of different compositions to be sensitive to 3 different spectral regions, or colors, 3-5 μm , 8-14 μm and 16-22 μm . The layers of material were very thin ($<10 \mu\text{m}$) and were joined together by an infrared transmitting epoxy. The method of manufacture involved picking a bulk piece of HgCdTe of the right spectral response and using that as a substrate on which to build the other colors sensitive elements. Each element measured 0.25 mm x 0.25 mm and there were six elements in the array. The longer wavelength region detected was 9.9 μm to 11.8 μm and the shorter one was 8.3 μm to 8.9 μm . The detector performance at 95 K was $3.5 \times 10^9 \text{ cm Hz}^{1/2}\text{W}^{-1}$ for the short wave part and $9.6 \times 10^9 \text{ cm Hz}^{1/2}\text{W}^{-1}$ for the longer-wave part, and the resistance of each element was 270 Ω .

The feasibility of 2- and 3-color detectors was shown to be possible with good performance and narrow band spectral response. Progress must be made in cutting down interface losses before the full potential of N-color HgCdTe detectors can be realized.

7. THERMAL IMAGING

7.1 REFERENCE TEMPERATURE DEVICES

A useful device in real-time thermal imaging where pictures are presented on an oscilloscope screen is a thermal reference system, or heated bar, with a linear temperature gradation from black to white, which can be shown along with the target on the screen, that will give a one to one correspondence between the intensities. Such a device was reported by J.A. Charles and J.E. Francis (22). This has the advantage over the hohlraum type of blackbody in that it provides a continuous range of reference temperatures. A one-dimensional fin was constructed. The differential equation for such a

fin is

$$\frac{d}{dx} [kA \frac{dT}{dx}] - h dA_s (T - T_\infty) - \sigma \epsilon dA_s (T^4 - T_\infty^4) = 0$$

where T = local fin temperature

h = convective film coefficient

T_∞ = room temperature

x = position down fin

and σ and ϵ have their usual values. Since the fin was insulated on one side dA_s , the area element, reduced to $w dx$ where w was the width of the fin.

A linear temperature profile

$$T = ax + T_r$$

where a was a constant and T_r the root temperature of the fin was introduced as the boundary condition and the equation then was reduced to dimensionless form.

The resulting equation for the fin thickness must be solved numerically.

An aluminum fin was constructed and a heater inserted into a hole drilled into the roof of the fin and cemented with heat-conducting glue. Thermocouples were embedded at regular intervals in the fin and Nichrome wire embedded one inch apart which could be heated to produce a visible scan on an infrared scanner. Thus a temperature on a thermograph could be compared quantitatively with this standard.

Another temperature measurement device is described by S.H. Praul and L.V. Humurcik (23). Thermocouples and thermometers require several seconds to come to equilibrium and are thus not very useful when it comes to measuring rapid changes in temperature. This paper describes a fairly simple device constructed to overcome this problem. A thermocouple was the basis of the device but the innovation was in the electronics. A step rise in temperature at the thermocouple gave a voltage rise

$$V(t) = V_0 (1 - e^{-t/T})$$

where V_0 corresponded to the voltage after infinite time at T was the time constant of the thermocouple. The differential equation describing this was written

$$V_0 = V(t) + T \frac{d}{dt} V(t).$$

This differentiation was performed easily by an RC network where $t \gg RC$. The network voltage R was amplified and added to $V(t)$.

Tests were made over a wide range of time constants ranging from 10 to 100 ms and RC set at 100 μ s. Actually, like other infrared detectors, the device measures emittance ($\epsilon \sigma T^4$) and not temperature directly.

7.2 THERMAL IMAGING SYSTEMS

In a paper by R. Bowling Barnes (24) the infrared imaging of the human body is discussed. In the introduction the radiative properties of blackbodies and real bodies are described. All bodies radiate energy but at the ambient temperature for humans, the wavelength of maximum emission lies in the infrared at $10\text{ }\mu\text{m}$. It was observed that as "incandescence" is defined as "glowing due to heat", all objects are infrared incandescent. The infrared radiation emitted by objects contains information about the object's temperature, emissivity, composition, etc.

An infrared camera was described (25). Infrared radiation emitted by a source fell on a scanning mirror and was then focussed on a thermistor heat detector. A mechanically rotated chopper intercepted the energy beam 200 times a second to compare it with a standard reference blackbody. By means of the thermistor, the incident infrared radiation was converted into an electrical signal, amplified, and used to drive a glow modulator tube which presents a display with visible light. This image was then recorded on film. Each display was calibrated by a quantitative thermal gray scale displayed on each thermogram. The device had several white-to-black scales ranging from 187°F to 1°F . The total scan time was 13 minutes, so that the presentation was not in real time.

The human body is an ideal subject for thermography. As the skin has been found to have an emissivity of almost unity in the 3 to $15\text{ }\mu\text{m}$ band, the intensity of the infrared radiation emitted can be equated directly with the temperature distribution across the target.

At wavelengths shorter than $2\text{ }\mu\text{m}$ the skin is fairly transparent to visible light and near infrared radiation, and there are thus great differences in absorption and reflection properties of the skin in this part of the spectrum. Thermograms of subjects from four different races were shown to illustrate this. The short wave radiation was excluded by means of a germanium lens which was completely opaque for wavelengths $<2\text{ }\mu\text{m}$ and highly transparent in the band $2\text{--}15\text{ }\mu\text{m}$. Thus these thermograms were true thermal pictures of the subjects. Even though the average human body temperature is 37.0°C , the surface temperature of the skin varies quite widely as a result of ambient temperatures, environmental conditions and body metabolism. When the many outside variables are standardized or known, the skin temperature may be used as an aid to medical diagnosis. As the skin is such a good emitter, any foreign substances on the skin will not alter its emissivity (unless, the substances are present in sufficient quantity). Thus it is usually not possible to create spurious hot spots.

Some thermograms were displayed showing the effects of fatty tissue (producing cold spots as fat is a poor thermal conductor) and skin over bony extremities which also produced cold spots because of the absence of highly

vascular tissue just beneath the skin surface. Some previous work is reported on the diagnosis of carcinoma of the breast, but the author reports some other interesting cases: An inflamed appendix, a breast cancer and an arterial occlusion in the leg of a 68-year-old man. In the latter case, the thermogram showed a 7°F temperature difference between the legs below the knee.

Some of the actual instruments used in medical radiography are described in a paper by W.L. Wolfe (25). It was observed that the minimum detectable temperature difference and the time constant of the system were the two most important quantities.

The first device described was the Thermograph T-1 built by the Barnes Engineering Co. This incorporated a reference blackbody and a mechanical chopper and a thermistor or lead sulfide element. Another device, the "Reconofax", built by H.R.B. Singer was used in aerial reconnaissance; this did not have an internal reference source.

A scanning system marketed by Westinghouse views a field of view of 90°. This system used a four-sided mirror and a lead sulfide or lead telluride element.

Another method of scanning, this time in image space, was with a Nipkow scanner. This was a rotating disk with holes or lenses in it in the shape of an involute which allowed light to pass through. Thus a raster was generated as the disk rotated. This device was used in early television sets.

Also described was a non-scanning device called an Evaporograph. An optical arrangement formed an image of the object on a membrane. The other side of the membrane was coated with a thin film of oil. The infrared radiation caused varying rates of evaporation of this film, so that the film had differing thicknesses over its area depending upon the intensity of the radiation. White light was then viewed through the membrane and the differential interference of the white light produced a color representation of the temperature distribution.

An interesting, non-technical review paper, covering the same ground as the previous few papers may be found in "Science Journal" (26).

A good analysis of the quantum detector type of thermal imaging system was described by S. Borg (27). In this paper the capabilities of the AGA Thermovision fabricated in Sweden were described. The apparatus consisted of a camera unit and display unit. The detector was photovoltaic indium antimonide cooled by liquid nitrogen to 77 K. The scanning was performed by means of an eight-sided prism scanning 8 lines per second. The prism rotated at 200 rps resulting in 1600 scanned lines per second. The 100-line picture thus appeared on the oscilloscope screen at 16 frames s⁻¹. The picture size was 50 mm x 60 mm. The temperature resolution was 100 picture elements per line. When photographs were taken on the display, many frames could be taken, thereby integrating out some of the noise and reducing the granularity of the picture.

Various models of camera are available, all using the same display. The main variations are in the field of view available, 10° x 10° being incorporated into the latest model. The temperature ranges available extend

from 1°C to 200°C with the level anywhere between -30°C and +200°C. Also available are isotherm controls. These displayed on the screen a uniform white area for all areas at the same temperature. The isotherms could be moved around and the difference in temperature determined from the change in the position of the isotherm marker in the gray scale displayed beneath the picture. This allowed an accurate, quantitative measurement of temperature.

Recording is usually done on Polaroid film. However, magnetic tape could be used. The tape had the advantage that it can be played back, stopped at any frame, and mapped with isotherms when convenient.

The thermal and spatial resolution of the system depends very much on all the optical parameters, amplifier characteristics etc. If the scanning speed of a system was increased, the upper frequency limit was increased producing a corresponding wider bandwidth. This in turn increased noise and decreased the resolution. However, there was a net improvement in resolution as the increased frequencies involved with higher scanning speeds reduced the 1/f detector and preamplifier noise. Also, when producing a Polaroid print of the oscilloscope display, the superposition of many frames increased the resolution.

A short discussion of the uses of the thermal imaging system in non-destructive testing was included in the paper by Borg.

Another paper dealing with thermal imaging of the natural environment is entitled "Infrared Images of Natural Subjects" (28). This paper contains a description of aerial imaging of some river systems in the industrial parts of Michigan state.

The equipment used was a Bendix thermal mapper, chosen so that it could be used easily from a light, single-engined aircraft. Recording was carried out using 70-mm film which was processed directly on landing. The scanning mechanism consisted of a rotating mirror scanning a 3-mrad-wide strip transverse to the aircraft motion, that motion supplying the sequencing of the strips to build up a picture. The detector produced video voltages which were processed and used to drive a glow modulator tube. The signal resulting from this was focussed and scanned across the film.

An infrared image of a portion of the Detroit river was taken at 8.15 pm in the 3.7 to 5.5 μ m band. Strong temperature contrasts in the water were easily visible and they were due to hot effluvia from factories and industries. Differences in temperature up to 10°C were common. Smoke stacks and factory building appeared substantially hotter than the natural surroundings. Another picture of the region near St. Augustine, Florida showed a similar, but much smaller, temperature contrast between inland water and tide-water from the ocean. Here the difference was about 1°C. This picture was taken in the morning when the trees and vegetation remained cool. The paper concluded with a discussion of the infrared properties of vegetation and chlorophyll.

8. APPLICATIONS OF THERMAL IMAGING

8.1 MEDICAL DIAGNOSIS

One of the various uses of thermal imaging is that of diagnostic assistance in medicine. R.N. Lawson and M.S. Chugtai (29) describe the relationship of breast cancer and body temperature. A typical rise in skin temperature above a cancer was 1°C . Of the 19 cases reported, 17 showed a temperature rise 1°C or more over the site of a cancer. Two did not show any rise. Out of 35 cases of benign lesions, 13 showed a slight temperature rise ($<0.5^{\circ}\text{C}$) while one showed a drop in temperature of 0.2°C . It was clear that carcinoma cells divide at a higher temperature than do ordinary body cells. It has been shown by other workers that certain animal tumours regressed when subjected to a degree of hyperthermia that was not lethal to host structures.

Although very helpful as a medical tool, it is unfortunate that infrared emission from the body is strictly a surface phenomenon for any change in skin temperature is a result of various internal processes (cancer, vascular disease) raising or lowering the ambient temperature at that site.

To enable any accurate diagnosis to be performed, the optical properties of the skin have to be known.

Many infrared cameras now use either indium antimonide or mercury cadmium telluride chips as the sensitive element. A paper by Jaeger (30) et al. discuss the relative abilities of these two compounds in the detection of low contrast targets. Indium antimonide responds to the $4.5 - 5.5 \mu\text{m}$ band and mercury cadmium telluride to $8 - 13 \mu\text{m}$.

The sea background noise was a function of sea state, cloud cover, sun position etc. Atmospheric attenuation, which reduced radiance difference between the target and background, was due mainly to scattering by fog and absorption by water vapour. Previous experiments have shown that attenuation is greater in the $5 \mu\text{m}$ band.

Measurements were made with a two channel infrared radiometer and were carried out from the Southern Coast of Norway, 30 m above sea level. The target was a 12.5 m fishing boat at distances of 10 - 15 km from the coast and was scanned at intervals of $1/2 \text{ km}$. Signals, noise and signal-to-noise ratios were plotted as a function of range.

All curves displaying signal-to-noise ratios showed better detection performance for mercury cadmium telluride particularly at ranges above 3 km.

At a signal-to-noise ratio of 2 the range of the mercury cadmium telluride system was approximately twice that of the indium antimonide system. As the sea background noise dominated all other noise sources detectors with higher detectivities would not have given higher signal-to-noise ratios. This would not be true had detector noise been dominant.

The authors concluded that the mercury cadmium telluride system sensitive in the 8 - 13 μm band was generally superior to the indium antimonide detector sensitive to 4.5 - 5.5 μm for the reason that the radiance of natural objects is greatest at 10 μm and atmospheric transmission is better in this range.

Infrared thermography is now used extensively in medicine in the diagnosis of various diseases such as breast cancer. A malignant tumor will produce a 1°C - 2°C rise in temperature at the surface of the skin and this is quite enough to be detected easily by modern infrared scanners. However, for small areas resolution becomes a problem. This has been analyzed by D.J. Macey and R. Oliver (31). They found that the rate of signal rise at a temperature discontinuity was determined by the time constant of the detector and its associated circuitry. The image signal rises after encountering the front edge of the discontinuity and fall after leaving it. For narrow regions, the signal may not rise to the time level.

A standard blackbody source was set up with a piece of card with vertical slits cut in it of widths from 2 mm to 20 mm. An AGA Thermovision camera scanned this object. With a field width of 330 mm, temperature discontinuities of widths of 6 mm or less showed significantly less than the true value. This deficit in the apparent temperature was found to be independent of background temperature and temperature excess and dependent on the scan rate and time constant of the circuitry. Thus for small areas significant temperature differences may be underestimated and so may not be detected. This would be important in clinical practice as a temperature difference of 1°C or 2°C is regarded as significant and a source (e.g. a vein) with a 3°C temperature excess would appear less than 1°C hotter than the background. The minimum dimensions for reasonably accurate measurement were given by two line elements horizontally and two line widths vertically corresponding to about 2% of the full dimension. These standards, achieved in all the presently available equipment, were considered adequate for current clinical needs.

Another paper by W.H. Sutherland (32) describes a device called a "Pyroscan" used in medical diagnosis. In this device a plane mirror scanned the image horizontally and vertically and projected the images onto an In Sb cell cooled to 77 K. Each picture was built up of 200 to 600 lines in a time that varied from 45 to 210 seconds. Clinical abnormality was shown up by the appearance of features absent from the "normal" thermography - a procedure similar to radiography. However the daily and individual variations in thermal contrast were greater than for an equivalent radiograph resulting in increased difficulty of interpretation. As a result of this it was found that the most useful information was gained by obtaining scans of discrete lines across a target at regular intervals and producing a set of temperature profiles. This method produced more accurate temperature values as comparison with standard sources of known temperature was much easier.

The Pyroscan produced a 0-to-30-V-dc output accurately proportional to temperature. For profile scanning, this voltage was fed into a recorder. For positioning the scan on the target, light beams were projected back through the optical system which appeared as bright spots on the target. The spot being investigated lay directly between these two points. The scanning of all temperature profiles was performed at a fixed sensitivity so that the recorder calibration corresponded to 1°C m^{-1} . The calibration could be checked anytime with three standard blackbody sources kept at 27, 32 and 37°C . The results consisted of thermograms and temperature profiles. For quantitative interpretation, the latter were much preferred as direct comparisons between different body areas were less confusing. Hot areas could be assessed more easily by averaging areas under the curves. The machine has been used extensively in the diagnosis of breast cancer.

8.2 DESIGN OF ARCTIC CLOTHING

The use of infrared radiometry to assist in the design of cold weather clothing has been reported (33).

To investigate radiative heat losses from the body, a Barnes I-8A scanning infrared radiometer was used to observe subjects standing 35 feet away in a natural environment. The device was sensitive to radiation between 1.8 and $10\text{ }\mu\text{m}$ and the output was recorded on Polaroid film. On the film record there was superimposed a gray scale which enabled the operator to compare this temperature scale with areas on the subject of the same shade.

The radiometer was used to scan five nude subjects standing at rest in an environment of 0°C to -5°C until the skin temperature at any site on the body fell below 4°C . These sites were monitored by thermistors and particular sites were chosen because they were the coldest areas of the body. For comparison, the radiometer was used to scan five subjects wearing standard Arctic clothing outfits and mukluks with a view to determining heat loss by radiation. Here the ambient temperatures varied between 0°C and -35°C and the wind varied between 0 and 160 ft min^{-1} . Subjects had to remain very still as the scanning time required to complete the picture was 8 minutes. Although the surface emissivities of the materials were not known, this did not affect the comparative evaluations.

The results clearly indicated the areas of the clothing assemblies that lost heat most readily to the surroundings. Wrinkles in the clothing were very apparent and these formed the most noticeable feature of the infrared images. A fair amount of heat was lost through the mukluks along the sides and top of the feet where the inner duffle socks were compressed and had lost much of their insulating value.

As for the nude subjects, the nose, feet, hands and cheeks were all very much cooler than the rest of the body. The fat deposit around the waist was shown to produce a lower skin temperature owing to its insulative value and the heavy musculature of the thighs and lower legs did not maintain high skin temperatures despite moderate shivering. It was observed that radiative

heat loss from nude subjects depended upon vasoconstrictive activity of the vasculature, the location of the major blood vessels and the absence or presence of insulative tissue.

9. REFERENCES

1. T.P. Gill, Some Problems in Low-Temperature Pyrometry, J. Opt. Soc. Am., 47, 11, Nov. 1957, pp. 1000 - 1005.
2. D. Weber, Spectral Emissivity of Solids in the Infrared at Low Temperatures, J. Opt. Soc. Am., 49, 8, Aug. 1959, pp. 815 - 820.
3. G.W. Cleek, J.J. Villa, C.H. Halmer, Refractive Indices and Transmittances of Several Optical Glasses in the Infrared, J. Opt. Soc. Am., 49, 11, Nov. 1959, pp. 1090 - 1095.
4. P.S. MacDermott, R.L. Powell, E.R. Stack, Infrared Measurement of the Optical Constants of the Low Temperature Glass System of 30% Arsenic - 34% Sulfur - 36% Thallium. Infrared Physics, 1, 1961, pp. 167 - 174.
5. D.L. Stierwalt, Infrared Spectral Emittance Measurements of Optical Materials, Appl. Optics, 5, 12, Dec. 1966, pp. 1911 - 1915.
6. C.S. Williams, Discussion of the Theories of Cavity-Type Sources of Radiant Energy, J. Opt. Soc. Am., 51, 1961, pp. 564 - 571.
7. H. Buckley, On the Radiation from the Inside of a Circular Cylinder, Phil. Mag., S7, 4, 23, Oct. 1927 (Part I) and Phil. Mag. S7, 6, 36, Sept. 1928 (Part II).
8. E.M. Sparrow, L.V. Albers, E.R.G. Eckert, Thermal Radiation Characteristics of Cylindrical Enclosures. J. Heat Transfer, Feb. 1962, pp. 73 - 81.
9. J.H. McLerran, Infrared Thermal Sensing, Photogram. Eng., 33, 1967, pp. 507 - 513.
10. R. Elam, D.W. Goodwin, K.L. Williams, Optical Properties of the Human Epidermis, Nature, 198, 4884, June 8, 1963, p. 1001.
11. D. Mitchell, C.H. Wyndham, T. Hodgson, Emissivity and Transmittance of Excised Human Skin in its Thermal Emission Wave Band, J. Appl. Physiol. 23, 1967, pp. 390 - 394.

12. D. Mitchell, Measurement of the Thermal Emissivity of Human Skin in vivo, Physiological and Behavioral Temperature Regulation, Hardy, Gagge and Stolwijk (Ed.) 1970, Ch. 3, pp. 25 - 33.
13. H.F. Greenler, F.J. O'Neill, Radiant-Energy Reflectance of Men's Wear Colors, Textile Res. J., 17, 2, Feb. 1947, pp. 63 - 68.
14. M. Smollet, The Properties and Performance of Some Modern Infrared Radiation Detectors, Infrared Physics, 8, pp. 3 - 7, 1968.
15. B.R. Holeman, R.G.F. Taylor, An Introduction to Thermal Imaging, J. RNSS, 25, 3, 1970, pp. 118 - 126.
16. C.M. Cade, B.V. Barlow, Fundamental Design Principles for Thermographic Scanners, Sci, Prog. Oxf., 55, pp. 167 - 185, 1967.
17. J.S. Chivian, R.N. Claytro, D.D. Eden, R.B. Hemphill, Infrared Recording with Thermochromic Cu_2HgI_4 , Appl. Optics, 11, 11, Nov. 1972, pp. 2649 - 2656.
18. R.W. Astheimer, F. Schwartz, Thermal Imaging Using Pyroelectric Detectors, Appl. Optics, 7, 9, Sept. 1968.
19. P.S. Nayar, A New Far Infrared Detector, Infrared Physics, 14, 1974 pp. 31 - 36.
20. J.L. Lachambre, A Pyroelectric Energy Meter, Rev. Sci. Instrum., 42, 1, Jan. 1971, pp. 74 - 77.
21. H. Halpert, B.L. Musicant, N-Color (Hg,Cd)Te Photodetectors, Appl. Optics, 11, 10, Oct. 1972, pp. 2157 - 2161.
22. J.A. Charles, J.E. Francis, Design of a Thermal Reference System for use in Thermography, Rev. Sci. Instrum., 44, 3, March 1973, pp. 291 - 294.
23. S.H. Praul, L.V. Humurcik, Instantaneous Temperature Measurement, Rev. Sci. Instrum., 44, 9, Sept. 1973, pp. 1363 - 1364.
24. R. Bowling Barnes, Thermography of the Human Body, Science, 140, 1963, pp. 870 - 877.
25. W.L. Wolfe, Infrared Imaging Devices Infrared Medical Radiography, Ann. New York Acad. Sci., 121, 1964, pp. 57 - 70.
26. C.M. Cade, A.E. Hanwell, Thermal Patterns, Sci. J., Feb. 1966, pp. 62 - 67.
27. S.B. Borg, Thermal Imaging with Real Time Picture Presentation, Appl. Optics, 7, 9, Sept. 1968, pp. 1697 - 1703.
28. R. Blythe, E. Kurath, Infrared Images of Natural Subjects, Appl. Optics, 7, 9, Sept. 1968, pp. 1769 - 1777.

29. R.N. Lawson, M.S. Chugtai, Breast Cancer and Body Temperature, Can Med. Ass. J., 88, Jan 12, 1963, pp. 68 - 70.
30. T. Jaeqer, A. Nordbayhn, P.A. Stockseth, Detection of Low Contrast Targets at 5 μ m and 10 μ m: a comparison , Applied Optics 11, 8, August 1972, pp. 1833 - 1835.
31. D.J. Macey, R. Oliver. Image Resolution in Infrared Thermography , Phys. Med. Biol., 1972, 17, 4, pp. 563 - 571.
32. Temperature profile scanning - A more Quantitative approach to Thermography . Bio-Med Engineering 5, 10, Oct. 1970, pp. 493 - 500.
33. J.H. Veghte, Determining Arctic Clothing Design by Means of Infrared Radiometry, Military Medicine, March 1962, pp. 242 - 246.

APPENDIX AList of Symbols

T = Temperature
 σ = Stefan-Boltzmann Constant
 ϵ = Emissivity
c = Velocity of light
h = Planck's constant
k = Boltzmann's Constant
K = Kelvin
 μm = Micrometer
 $^{\circ}\text{C}$ = $^{\circ}\text{Celsius}$
 $^{\circ}\text{F}$ = $^{\circ}\text{Fahrenheit}$
Cu = Copper
Hg = Mercury
I = Iodine
In = Indium
Sb = Antimony
Te = Tellurium
s = second

DOCUMENT CONTROL DATA - R & D		
(Security classification of title, body of abstract and indexing annotation must be entered when the overall document is classified)		
1 ORIGINATING ACTIVITY Defence Research Establishment Ottawa National Defence Headquarters Ottawa, Canada K1A 0Z4		2a. DOCUMENT SECURITY CLASSIFICATION UNCLASSIFIED
		2b. GROUP
3 DOCUMENT TITLE THERMAL IMAGING FOR CLOTHING RESEARCH - A REVIEW OF THE LITERATURE		
4. DESCRIPTIVE NOTES (Type of report and inclusive dates) TECHNICAL NOTE		
5. AUTHOR(S) (Last name, first name, middle initial) HIDSON, D.J.		
6 DOCUMENT DATE APRIL 1976	7a TOTAL NO OF PAGES 33	7b NO. OF REFS 33
3a. PROJECT OR GRANT NO 79-01-04	9a. ORIGINATOR'S DOCUMENT NUMBER(S) DREO TECHNICAL NOTE NO. 76-13	
8b. CONTRACT NO.	9b. OTHER DOCUMENT NO.(S) (Any other numbers that may be assigned this document)	
10. DISTRIBUTION STATEMENT DISTRIBUTION IS UNLIMITED		
11 SUPPLEMENTARY NOTES		12. SPONSORING ACTIVITY
13 ABSTRACT <u>UNCLASSIFIED</u> This paper reviews the literature relating to thermal imaging (particularly real-time thermal imaging), photoconductive, photovoltaic and pyroelectric infrared detectors and the application of thermal imaging to the design of Arctic clothing. The application of thermal imaging to medical diagnosis and non-destructive testing is also discussed.		

KEY WORDS

TEMPERATURE MEASUREMENT

INFRARED DETECTION

ARCTIC CLOTHING

INFRARED CAMERAS

INSTRUCTIONS

1. ORIGINATING ACTIVITY Enter the name and address of the organization issuing the document.
- 2a. DOCUMENT SECURITY CLASSIFICATION Enter the overall security classification of the document including special warning terms whenever applicable.
- 2b. GROUP Enter security reclassification group number. The three groups are defined in Appendix 'M' of the DRB Security Regulations.
3. DOCUMENT TITLE Enter the complete document title in all capital letters. Titles in all cases should be unclassified. If a sufficiently descriptive title cannot be selected without classification, show title classification with the usual one capital-letter abbreviation in parentheses immediately following the title.
4. DESCRIPTIVE NOTES Enter the category of document, e.g. technical report, technical note or technical letter. If appropriate, enter the type of document, e.g. interim, progress, summary, annual or final. Give the inclusive dates when a specific reporting period is covered.
5. AUTHOR(S) Enter the name(s) of author(s) as shown on or in the document. Enter last name, first name, middle initial. If military, show rank. The name of the principal author is an absolute minimum requirement.
6. DOCUMENT DATE Enter the date (month, year) of Establishment approval for publication of the document.
- 7a. TOTAL NUMBER OF PAGES The total page count should follow normal pagination procedures, i.e., enter the number of pages containing information.
- 7b. NUMBER OF REFERENCES Enter the total number of references cited in the document.
- 8a. PROJECT OR GRANT NUMBER If appropriate, enter the applicable research and development project or grant number under which the document was written.
- 8b. CONTRACT NUMBER If appropriate, enter the applicable number under which the document was written.
- 9a. ORIGINATOR'S DOCUMENT NUMBER(S) Enter the official document number by which the document will be identified and controlled by the originating activity. This number must be unique to this document.
- 9b. OTHER DOCUMENT NUMBER(S) If the document has been assigned any other document numbers (either by the originator or by the sponsor), also enter this number(s).
10. DISTRIBUTION STATEMENT Enter any limitations on further dissemination of the document, other than those imposed by security classification, using standard statements such as:
 - (1) "Qualified requesters may obtain copies of this document from their defence documentation center."
 - (2) "Announcement and dissemination of this document is not authorized without prior approval from originating activity."
11. SUPPLEMENTARY NOTES. Use for additional explanatory notes.
12. SPONSORING ACTIVITY Enter the name of the departmental project office or laboratory sponsoring the research and development. Include address.
13. ABSTRACT Enter an abstract giving a brief and factual summary of the document, even though it may also appear elsewhere in the body of the document itself. It is highly desirable that the abstract of classified documents be unclassified. Each paragraph of the abstract shall end with an indication of the security classification of the information in the paragraph (unless the document itself is unclassified) represented as (TS), (S), (C), (R), or (U).

The length of the abstract should be limited to 20 single-spaced standard typewritten lines, 7½ inches long.
14. KEY WORDS. Key words are technically meaningful terms or short phrases that characterize a document and could be helpful in cataloging the document. Key words should be selected so that no security classification is required. Identifiers, such as equipment model designation, trade name, military project code name, geographic location, may be used as key words but will be followed by an indication of technical context.